Journal of Chemistry and Chemical Sciences, *Vol.12(2),28-42, February, 2022* *ISSN 2229-760X (Print)*
(An International Research Journal), *www.chemistry-journal.org* *ISSN 2319-7625 (Online)*

Droplet Investigation on Hydrophobic Artificial and Natural Surfaces: Molecular Weight and Viscosity of Polymer Effects the Droplet Distortion

Anand Khistariya[1*] and Ravi Tank[1]

[1]Department of Industrial Chemistry,
Atmiya University, Rajkot, Gujarat, 360005- INDIA.
[*]email: anand.khistariya@atmiyauni.ac.in

(Received on: February 18, 2022)

ABSTRACT

Contact angle measurement of water, benzyl alcohol, ethylene glycol and glycerol are performed on hydrophobic surfaces of six polymers and four natural surfaces. We performed drop impacts dynamic of water droplets on an artificial polymer hydrophobic surfaces and natural hydrophobic surfaces with different impact velocities. Highest spread length and oscillations were observed on both high-density polyethylene (MI 42) and polypropylene (Bolton) due to the Wenzel regime. Two impacts, sticking and deposition was identified on the polymer samples due to the low static contact angles. Rebound, splashing, fragmentation and vibrational oscillations were observed due to the micro scale roughness on the natural surfaces. Highest static contact angle of water droplet (86.2±2.1) and lowest viscosity was obtained on polyethylene (Mw 35k) surface. Lowest static contact angle (79.9±2.8) and highest viscosity was observed on polypropylene surface. Furthermore, highest static contact angle of water drop (118.02±7.46) was observed on Purple sage (Leucophyllum frutescens) surface and lowest static contact angle (98.38±4.91) was observed on Eucalyptus (Corymbia) surface. The viscosity and critical surface energy of the polymer samples were also measured and discussed.

Keywords: Natural and artificial hydrophobic surfaces, contact angle, Wenzel effect, Viscosity, molecular weight, water droplet behaviour.

1. INTRODUCTION

The contact angle for a liquid droplet on a surface is commonly used to characterise wettability of the surface. Literature reveals that there are two models that illustrates wetting

phenomenon of the superhydrophobic surfaces one is Wenzel's model and other is Cassie-Baxter model[1,2]. Wenzel model (Robert N. Wenzel 1936) describes the homogeneous wetting fact while Cassie-Baxter model is needed when the surface is heterogeneous. Moreover, various polymer surfaces PMMA (poly methyl methacrylate) and PET (polyethylene terephthalate) have been used to determined contact angles[3]. Balkenende *et al.*, have measured contact angels of various liquids using formula[4].

The ability of water to bounce on superhydrophobic surface provides an indication of surface roughness, high contact angle and extreme water repellent properties. The various approaches (bounce, splash, fragmentation and so on) generally depends not only the volume of the droplet but also the surface tension and dynamic velocity. In addition, the surface wettability associated mainly of the surface energy and geometrical structure of the solid surface. Jung *et al.*,[5] reported that dynamic effects such as the bouncing and splashing of a droplet can affect the solid-air-liquid interface of the surface. Due to the internal force and certain pressure of a liquid droplet, the transition occurs between solid-air-liquid interfaces to a solid-liquid interface. The highest static contact angles were achieved for micro- and hierarchical structures were 154º and 169º respectively. Furthermore, rough surfaces also obtained by photolithography technique[6]. Jung and his team has fabricated micro-patterned surface with single-crystal silicon (Si) using photolithography method[7]. The nano patterned surfaces were fabricated by Poly(methyl methacrylate) (PMMA) with both low aspect ratio (LAR) and high aspect ratio (HAR) using soft lithography. To increase the hydrophobicity of the surfaces, a SAM of perfluorodecyltriethoxysilane (PFDTES) was deposited on the sample surfaces using a vapour phase deposition technique[8].

Combination of ethanol and PVC (poly vinyl chloride) is widely used to form superhydrophobic materials[9]. The formed PVC surface become rougher with the increase of ethanol content (<50%) in the PVC solution, and more pores and nano-composites are formed[10]. Roch *et al.*, formed silane with an alkyl group to present a hydrophobic character and glycidyl functional group allowing the formation of strong bond between the surface groups and the coatings of the cotton fibres. This phenomenon will increase durability of superhydrophobic surfaces[11]. Superhydrophobic surfaces can also be produced by chemically depositing on the polymer surfaces. The plasma-enhanced chemical vapour deposition (PECVD) has recently widely used and famous method (with arrangement of Ag/TiO2) to produce superhydrophobic surfaces[10].

Leaves of some plants, notably the Lotus flower leaves, have this property as an essential part of a self-cleaning mechanism[12]. The application of this mechanism is desirable also for non-biological systems, such as windows, painted exterior surfaces, and so on[13,14]. The natural superhydrophobic surfaces have micro- and nano-structure which is responsible for bouncing of water droplet and high contact angle due to its roughness and structure. Recently, there is a significant amount of work has already been done to study wetting surfaces whether it is a natural or an artificial. Furthermore, many methods are available in literature to create superhydrophobic surfaces with different approaches are enthused by the "Lotus effects"[12, 15]. Surface roughness and its structure play a very important role to produce surface hydrophobic.

Lotus leaf (Nelumbonucifera) being the standard example to define hydrophobicity of surfaces and thus, it is extremely difficult to wet. Lotus has been a symbol of purity in some religion since many years due to its hydrophobicity. Yan *et al.*,[10] have demonstrated that Taro (Colocasiaesculenta) leaves and India canna (Cannageneralis bailey) are superhydrophobic in nature due to their structures. To understand the superhydrophobicity of surfaces, there are two models i.Wenzel and ii.Cassie–Baxter is well known, from the equations we can understand the relation between the surface roughness and wetting phenomenon. Surface roughness and low surface energy of materials also play an important role to understand superhydrophobicity of surfaces. Koch *et al.*,[16,17] suggested hierarchical sculptures in Salvinia leaves which foams hydrophobicity with the creation of air pockets. Some leaves protect itself from environment and organisms such as lotus leaf due to its hierarchical levels. In addition, advanced research has indicated that the plant cuticle and leaf waxes are important features to make surface rough.

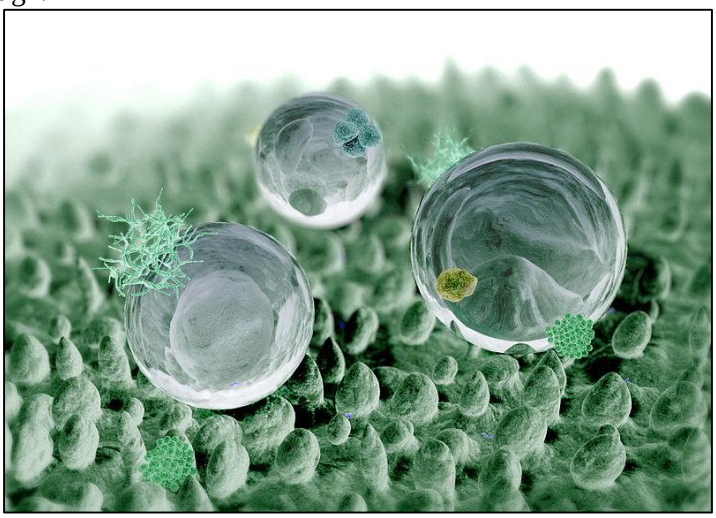

Figure 1. Water droplet on lotus leaf structure.

The figure 1 represent the high contact angle (>150^{o}) of water droplet on lotus leaf surface. On such surfaces, the physical adhesion forces between the particle and the surface are very less therefore water droplets and other dust particles roll off the leaves. Hence, lotus leaves clean their surface according to above phenomenon with high static and hysteresis contact angle[18].

There are not only plants surfaces having hierarchical structure and roughness to produce superhydrophobicity but also there are some species of insects, for instance their wings, legs and so on shows superhydrophobicity. Nowadays biomimetic is becoming an effective approach to develop superhydrophobic surfaces in nature. Many animals have capabilities to remove water from their skin. The one example of such an animal is water striders that can move and stand on water surfaces using their hydrophobic legs[10]. The Nano sized grooves on leg produce hydrophobicity and it makes them to stand effortlessly and move

quickly on water surface[19]. For example, Orthoptera Acridacinereacinerea (Thunberg), Hymenoptera Vespa dybowskii (Andre), and DipteraTabanuschrysurus (Loew) have multi-scale hierarchical roughness and identical structures enhance the superhydrophobicity on the wings with high contact angle[20,21].

Only a few studies have shown the effect of the impact of a water drop on both polymer and natural hydrophobic system. As mentioned above some most important natural and artificial methods to coat surfaces, to increase contact angle and to increase roughness of surfaces for industrial applications. In this context we have studied super hydrophobicity of six artificial polymer, Polyethylene (PND 33-300), Polyethylene MI=42 (high density), Polyethylene (Mw=35k), Polypropylene, Polypropylene (Bolton) and Polystyrene and four natural surfaces such as Leucophyllum frutescens (Purple sage), Lactuca virosa (Wild lettuce), Montbretia (Crocosmia) and Corymbia (Eucalyptus) for industrial applications.

2. MATERIAL AND METHODS

The hydrophobic polymer samples such as Polyethylene (PND 33-300) from UniPetrol and Polyethylene MI=42 (high density) 428019, Polyethylene (Mw=35k) 427799, Polypropylene 428116, Polypropylene (Bolton) Moplen HP561R and Polystyrene 00926 were purchased from Sigma-Aldrich, India. All solvents used to measure contact angles and critical surface energy of solids without further purification. Such as, Benzyl alcohol 100516, Ethylene glycol 107211 purchased from Sigma-Aldrich, India and Glycerol 56815 from Alfa-Aesar. Distilled water was used from laboratory. All hydrophobic leaves have been used to measure drop impacts and contact angle measurement, Leucophyllum frutescens (Purple sage), Lactuca virosa (Wild lettuce), Montbretia (Crocosmia) and Corymbia (Eucalyptus) were collected from local region.

2.1 Injection module method to prepare samples

Sample preparation was carried out using injection module method at different temperature. Various bone-shapes and square plates were prepared from raw material of the samples. Polyethylene (high density) and Polyethylene (Mw=35k) were prepared at ~180 ^{0}C and Polypropylene and Polypropylene (Bolton) were prepared at ~200 ^{0}C, whereas, Polyethylene (PND 33-300) and Polystyrene were prepared at ~250 ^{0}C.

2.2. Surface characterisations

2.2.1. Rheological experiments of the polymer samples: Rheological experiments were carried out using a Bohlin C-VOR equipped with a Peltier device for temperature control. The measurements were performed by using a cone-plate measuring system, which works by sandwiching a small amount of fluid within a rotating cone and a fixed plate. A cone spindle of diameter 40nm and a cone angle 4^0 was used during the experiment. A round shape tested sample was placed on the cone plate and then the upper cone plate was set at measured (usually

in µm) distance. The measurements were performed in viscometry-controlled mode with shear strain of 0.1 and a steady shear rate (1/s) 0.02. The measurements were monitored in the rheometer at 170 ^{0}C to 250 ^{0}C range for six different samples up to the fix time. Afterwards, the results and graphs were collected and saved in the computer for further analysis.

2.2.2. Contact angle experiments: The contact angle measurements were carried out on the surface of different polymer and natural samples with four test liquids. A 25mm x 25mm size of square polymer plate and four hydrophobic plant leaves were placed onto the angle measurement device. Approximately 8µL liquid drop was positioned onto the middle of the tested sample surface. Then, the drop picture was taken and analysed by the IC capture 2.2 software and the contact angle was measured by the Image J launcher software. Experiment repeatability was achieved by running measurements with at least four cycles with every single sample and liquid. Critical surface energy was measured with tangent model from contact angles data, which were obtained from the experiments. The contact angle was calculated from the Young-Laplance equation.

2.2.3. Surface analysis by digital microscopy: Surface morphology of the natural samples was characterised at microscopic level. Digital microscopy was used to analysed leaf roughness, hair and wax**.**

2.3. Experimental setup

In order to test bouncing behaviour of water droplet, an advanced-built apparatus was used to regulate the flow of water, as well as record and store the videos. The setup comprises of two main portions, the physical assembly to hold the camera and microliter syringe and needle, which is shown in the figure 2.

Figure 2. The droplet measurement assembly, with high-speed camera.

The water drop experiment was performed in the central instrumentation facility laboratory at Atmiya University. As shown in figure 2, an adjustable microliter syringe has been set steady at 25mm and 70 mm distance above the targeted samples; distance has been raised to affect the impact velocity. The syringe-needle was controlled physically by pressing down to release a single drop of water. This required moderate patience as the syringe favours to expend a small stream. For recording the dataset, a movable high-speed camera, Casio Exilim EX-FH20 with recording speed up to 1000 fps and 20x optical zoom, Image J software, Virtual Dub Portable software and a high voltage lamp were used. The provided camera was placed at a fixed distance and height to the contact surface. Manual focus and zoom were used to adjust the suitable video capture quality. For the experiments, the camera was set to 420 fps to record the water drop experiments. For these high frames per second recording, a large lamp was used to provide suitable light for each frame. A high-speed camera and an appropriate assembly were able to record the instants before and after the impacts of the water droplet on particular sample surface, which could later be possible to analyse each frame by Image J, Virtual Dub Portable software and a computer assembly.

The software programs Image J and Virtual Dub Portable were used for analysis of the data and understand the impacts frame by frame. Virtual Dub Portable software enables to analyse the video by each frame (in terms of droplet behaviour. For instance, splash, bounce, oscillation and fragmentation) and it was possible to extract particular images from the video. Then Image J software was used to measure the spread length, drop height and distance of the water droplet. Generally, length, height and oscillations were measured by the measuring pixels of the image.

3. RESULTS AND DISCUSSIONS

3.1 Rheological experiments

Rheology study carried out to measure the effect of temperature and viscosity on polymer samples. As shown in figure 3, viscosity of higher molecular weight polyethylene (35k) was very low and constantly decreases with increase on temperature. However, high-density polyethylene (MI42) was started melt down at <150 ^{0}C and appeared relatively low viscous than polyethylene (PND 33-300). Munstedt and Auhl[22] have showed the shape of the viscosity curves depends on the polymer chain and molecular structure of the tested sample. In fact, viscosity measurement experiments are very sensitive towards the temperature phenomenon and such type of rheological experiments can preferably be used for a molecular characterisation of polymers.

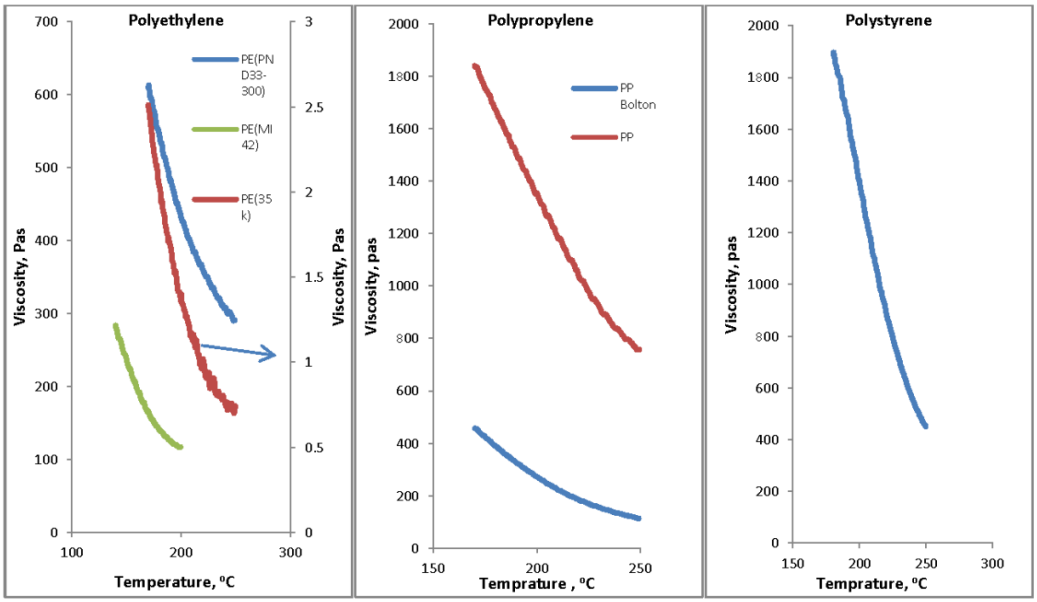

Figure 3. Viscosity vs. temperature plot of the three different polymer samples.

It was observed that polypropylene samples simply act very thicken during the experiment compare to polyethylene samples (figure 3). Both samples polypropylene and polypropylene (Bolton) were found highly viscous and melted at relatively high temperature. The viscosity of the initial polypropylene samples was very high at low temperature.

In addition, above relationship determines by the Arrhenius equation, in which at higher temperatures, the collision between two molecules probably the higher. The higher collision rate results in a higher kinetic energy, which has an effect on the activation energy of the reaction[23, 24].

Thus, Arrhenius equation is: $k=A \exp(-Ea/RT)$

Where, k is the rate coefficient, A is a constant, Ea is the activation energy, R is the universal gas constant, and T is the temperature (in kelvin).

Figure 3 shows, polystyrene seemed nearly same viscous as polypropylene. On initial run, it behaved highly viscous as shown in the graph, later viscosity was decreased with increasing the temperature. The relation between the viscosity and the contact angles of the samples is obvious. The contact angles on highly viscous materials have been studied in many literatures. Keller *et al.*,[25] have studied the effect of advancing velocity and liquid viscosity on the dynamic contact angle between a solid surface and various hydrocarbons. They have tested two silicon oils and hydrocarbons and as a result, advancing contact angles for viscous oils was up to two times higher.

3.2 Contact angle measurement and the critical surface energy of the polymer samples

The contact angle measurements and critical surface energy measurements were carried out on six polymer-tested samples with four tested liquids. The surface tension of benzyl alcohol, ethylene glycol, glycerol and water is 39 mJ/m2, 47.70 mJ/m2, 64 mJ/m2 and 72.80 mJ/m2 respectively. The measured contact angles are stated in table 1.

Table 1. Average contact angles of four solvents droplet on the tested polymer surfaces.

Sr. No	Sample	Benzyl alcohol	Ethylene Glycol	Glycerol	Water
1	PE(PND 33-300)	24.3	63.8	76.0	81.8
2	PE(MI=42)	25.9	69.9	78.4	83.4
3	PE(Mw=35k)	41.7	73.6	79.4	86.2
4	PP	27.2	68.3	73.9	79.9
5	PP(Bolton)	25.9	65.6	71.2	74.6
6	PS	21.8	54.0	66.0	81.8

The highest static contact angle was obtained on the polyethylene (Mw=35k) surface with all tested liquids. Our contact angle data on PE surfaces nearly agrees well with the previous literatures data[4]. However, comparatively low static angle was obtained on all polymer samples because of the Wenzel regime. Callies and Quere[26] have identified that due to the small pillars on the fibrous surface; a water droplet usually shows Wenzel regime, however, with increasing the height of the pillars will favour the Cassie state. Here contact angle data has been used to evaluate drop impacts on the surfaces and critical surface energy of tested samples. It is widely accepted in many literatures that the highest static contact angle allows a water droplet to rebound from the surface[5,7].

3.3 Surface characterisation

Critical surface energy of polymer surfaces has been measured via tangent model (Y= mx+c approach). The graphs have been plotted against the surface tension (YL) of measured liquids and cosine (Cos θ) of the average contact angles, which is given in figure 4.

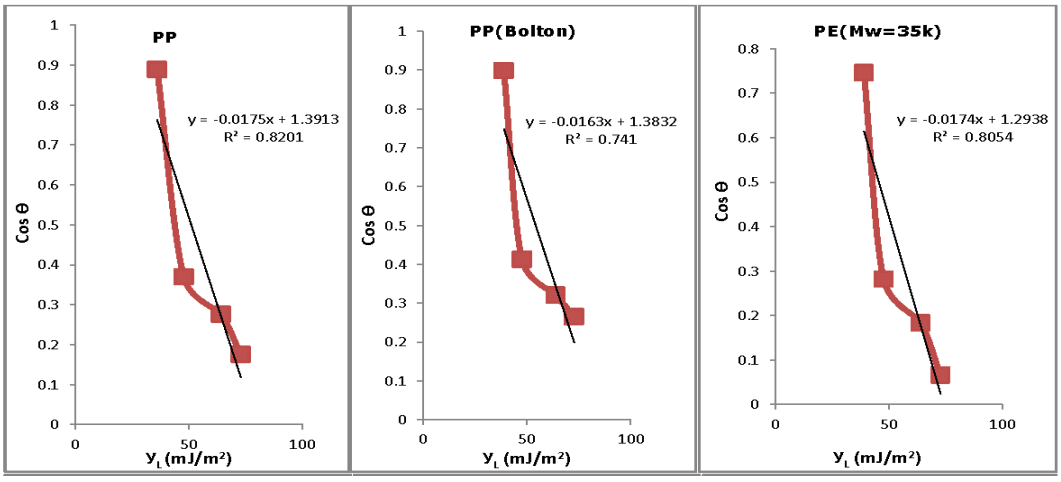

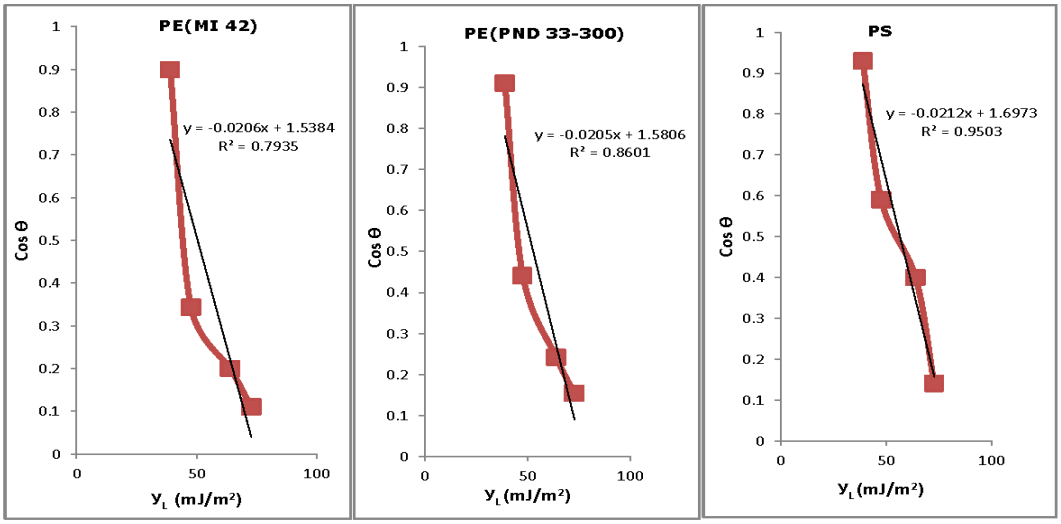

Figure 4. Contact angles on tested polymer surfaces plotted as Cos θ vs γ_L.

Figure 4 indicates that ethylene glycol (YL=47.7 mJ/m2) fluctuated more than other liquids at some point. Therefore, surface tension of ethylene glycol was measured by Du Noüy–Padday method for further analysis. Surprisingly, obtained results were similar to those available in literature results. Three experiment runs were carried out at room temperature (22 ^{0}C) and obtained results are 47.8, 47.7 and 47.7 mJ/m2, respectively. The data are given in table 2.

Table 2. Critical surface energy of solids with and without ethylene glycol for comparison

Samples	Ys mJ/m2 (with ethylene glycol)	Ys mJ/m2 (without ethylene glycol)
PP	22.36	29.92
PP(Bolton)	23.50	32.98
PE(Mw 35k)	16.88	26.26
PE(MI 42)	26.13	34.05
PE(PND 33-300)	28.32	34.37
PS	32.89	36.31

3.4 Contact angle measurement on the natural samples

Contact angle measurements were carried out on four hydrophobic leaves using water. The contact angles on micro structure leaves such as Crocosmia (Montbretia), Eucalyptus (Corymbia), Purple sage (Leucophyllum frutescens) and Wild lettuce (Lactuca virosa) are 107.50±1.96, 98.38±4.91, 118.02±7.46 and 107.31±0.88 respectively.

As shown in figure 5, highest static contact angle among others leaf was achieved on Purple sage (Leucophyllum frutescens) surface. According to Koch *et al.*,[17] a water droplet on particular leaf shows Cassie-Baxter regime because of the three-dimensional epicuticle waxes which enables a droplet to sit gently on the surface. In Purple sage (Leucophyllum frutescens) same waxes were observed which is responsible for good static contact angle. However, the

lowest contact angle was identified on Eucalyptus (Corymbia) smooth surfaces. Under microscopy, small dots were observed which allows to droplet to form Wenzel regime. The transition between the wetted (Wenzel) and composite (Cassie) conditions is a direct consequence with the micro droplet radius proportional to the pitch over pillar diameter[27]. Zhang *et al.*,[28] have proposed that the static contact angle is not only just depending on the Cassie and Wenzel regime but also it be contingent on the volume of the droplet. Lesser then 4μL volume of water droplet would not be able to deposit on the hydrophobic surface because of the low adherence of the surface.

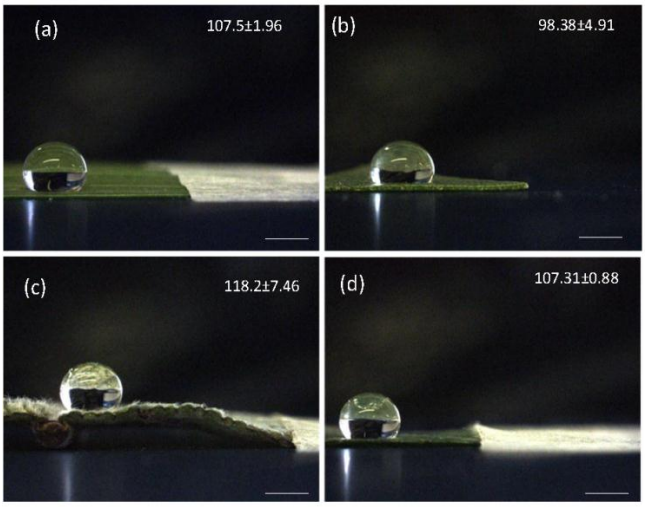

Figure 5. Water droplet resting on (a) Crocosmia (Montbretia) (b) Eucalyptus (Corymbia) (c) Purple sage (Leucophyllum frutescens) and (d) Wild lettuce (Lactuca virosa) surface. (Scale bar 1cm)

3.5 Drop impacts on the polymer samples

The impact experiments were carried out on polypropylene, polypropylene (Bolton), polyethylene (PND 33-300), polyethylene (MI=42), polyethylene (Mw=35k) and polystyrene which is considered as hydrophobic surfaces with approximately 8 μL water drop diameter. On the impact image sequences, two consequences such as deposition and sticking have been identified. The images of drop impact studies are given in supplementary (figure 7 to 11).

The different stages of drop during its impact on hydrophobic polymer surface are demonstrated by an example of sequence of snapshots existing in the figures. The water droplet was released at 25mm distance from the needle. As shown in the figures, due to small static angle, a droplet did not bounce off from the surfaces but initially it was sticking to the surface and then numbers of oscillations have been occurred in few milliseconds, which are presented in table 3. Minimum two times and maximum four times of droplet reformation have been noticed during each experiment. According to Rioboo *et al.*,[29] dynamic contact angles and contact angle hysteresis (CAH) are changing due to the oscillations of the droplet. Sticking regime has been noticed on all three polyethylene surfaces. In the beginning, droplet was stick

to the surface then reformation and oscillations occurred instantly. However, on polypropylene surfaces, instant reformation and number of oscillations have been identified which distinguished polyethylene from polypropylene.

Table 3. Spread length, oscillations and drop height were measured on six tested samples

Samples	Spread length (mm)	Oscillations	Drop height[a] (mm)
PE(MI=42)	0.80	13	0.40
PE(Mw=35k)	0.55	12	0.35
PE(PND 33-300)	0.75	8	0.25
PP	0.70	10	0.30
PP(Bolton)	0.65	14	0.30
PS	0.70	12	0.35

[a]At the end of oscillations.

In summary, spreading length of the water droplet has been measured while the droplet deposited on the surface. Drop height was measured in the end of each experiment. Highest spreading length (0.80mm) as well as drop height (0.40mm) was obtained on polyethylene (high-density) surface. However, maximum oscillations occurred on polypropylene (Bolton) sample. Minimum oscillations and drop height were achieved on polyethylene (PND 33-300) and polypropylene surfaces. Moreover, less recoil has been observed on polystyrene surface. Indeed, it has been noticed that the sticking process was very fast and formed contact angle was comparatively low on polyethylene (PND 33-300) surface. The relation between critical surface tension of solids and the drop impacts are difficult to determine. Though, more oscillations and maximum spread length occurred on high density and high molecular polyethylene surfaces.

3.6 Drop impacts on the natural surfaces

The drop impacts were characterised on four superhydrophobic plants such as Leucophyllum frutescens (Purple sage), Lactuca virosa (Wild lettuce), Montbretia (Crocosmia) and Corymbia (Eucalyptus) using water.

The micro-scale and nano-scale structures, small micro sized hair, wax on the upper part of the natural surfaces enhance hydrophobicity. Thereby enabling droplets of water to roll off the leaf and remove dirt[21]. Many authors have introduced sculpturing in the plants and basic terminology has already been given in the number of literatures.

For the identification of leaf structure on micro level, leaf sample has placed under microscopy to evaluate its basic surface morphology (figure 6). The outline of wax, dots and hair on leaves are easily visible by electron microscopy. On Crocosmia (Montbretia) leaf surface, small horizontal lines are situated which are responsible for Cassie-Baxter regime and high contact angle. Furthermore, densely covered three-dimensional waxes on Purple sage (Leucophyllum frutescens) allows droplet to rest, which is also produced Cassie-Baxter regime and high contact angle. However, Eucalyptus (Corymbia) and Wild lettuce (Lactuca virosa) surfaces are almost similar. Surface roughness of the both structures appeared due to the growth of small dots, which is responsible for hydrophobicity.

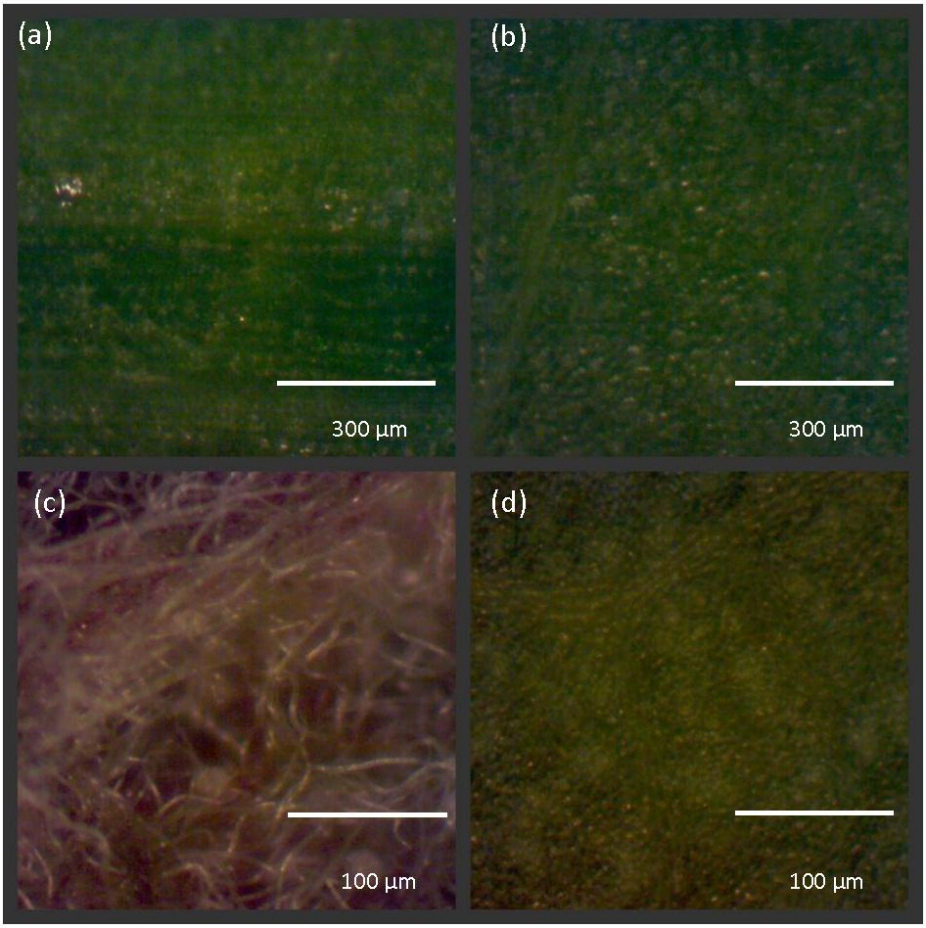

Figure 6. Microscopic images of the natural leaves. (a) Horizontal small lines were appeared on Crocosmia (Montbretia) leaf (b) On Eucalyptus (Corymbia) surface, small dots were observed (c) shows a brownish surface on Purple sage (Leucophyllum frutescens), which is densely covered with three dimensional waxes (d) shows Wild lettuce (Lactuca virosa) surface with tiny dots.

The static contact angle of the hydrophobic surfaces of Crocosmia (Montbretia), Eucalyptus (Corymbia), Purple sage (Leucophyllum (a) frutescens) and Wild lettuce (Lactuca virosa) were θ=107±1.96, 98±4.91, 118±7.46 and 107±0.88 respectively. Drop impact experiments were carried out with the distance 35mm and 70mm from the needle to sample surface. The images of drop impact study are given in supplementary (figure 12 to 19). When a droplet imposes on a hydrophobic surface, different dynamic behaviour was found. From the less distance (35mm) or low impact velocity, regular vibrating elastic rebound was observed with a velocity almost equal to impact velocity. As the impact velocity was increased by the distance increased, droplet fragmentation was observed which was not observed on less impact velocity. Fragmentation resembles to the formation of various droplets due to impact pressure.

The behaviour of the resulting droplets still corresponds to a Cassie-Baxter regime[30]. In this case, retreating breakup and possibly splash are also observed.

At low impact velocity, there was not any rebound observed on the Eucalyptus (Corymbia) surface. In beginning of the experiment, deposition occurs when, after touching the surface, the drop was showed some oscillations and it stayed on the surface. However, Rebound and oscillations with intensive shaking and vibration were identified with high impact velocity.

On the Purple sage (Leucophyllum frutescens) surface, partial rebound and vibrating oscillations were found. Moreover, it was observed that the droplets were greatly elongated before taking off. As the velocity increased, water did not bounce off the surface. It was identified that the droplet broke into many satellite drops during spreading stage due to the higher impact velocity. This process called splashing when water droplet turns into the tiny drops due to the higher impact velocity. Chen *et al.*,[31] has demonstrated that splash occurs on dry and smooth surfaces because of the compressible stress from air, which tries to pull the liquid sheet upwards, and the stress of the surface tension.

4. CONCLUSION

We have examined static contact angle using four different solvents on polymer materials and water on natural surfaces. It has been observed that the lowest viscosity has a direct relationship with the contact angle. Thus, highest static contact angle of water droplet (86.2±2.1) and lowest viscosity was showed on polyethylene (Mw 35k) surface. Highest viscosity, however, is inversely proportional to the lowest static contact angle. Therefore, comparatively lowest static contact angle (79.9±2.8) was identified on high viscous polypropylene surface. Highest static contact angle (118.02±7.46) was observed on Purple sage (Leucophyllum frutescens) surface. Lowest static contact angle (98.38±4.91) was observed on Eucalyptus (Corymbia) surface. On other hand, further studies need to be made in order to increase the static angle and drop effects on such hydrophobic surfaces with the help of surface modification. Among all solvent, water shows maximum contact angle on both surfaces. Thus, we have chosen water as a solvent to study its droplet impact on surfaces, polymer and natural.

Droplet impact on artificial hydrophobic surfaces such as PP, PP (Bolton), PE (Mw 35k), PE (MI 42), PE (PND 33-300), PS and natural hydrophobic surfaces such as Crocosmia (Montbretia), Eucalyptus (Corymbia), Purple sage (Leucophyllum frutescens) and Wild lettuce (Lactuca virosa) was studied with an approximately 8 μL water droplet. Sticking and deposition regime was observed due to the small static contact angle on the polymer samples. Highest spread length and oscillations were observed on both high-density polyethylene (MI 42) and polypropylene (Bolton) due to the Wenzel regime. However, fewer oscillations were identified on polyethylene (PND 33-300) surface. Instant recoil and sufficient droplet spreading length was observed on polystyrene surface. Partially rebound and vibrational oscillations at low impact velocity were observed on Crocosmia (Montbretia) and Purple sage (Leucophyllum frutescens) surfaces due to the small micro dots and densely covered three-

dimensional waxes on the surfaces. Furthermore, fragmentation was occurred on Crocosmia (Montbretia) and Purple sage (Leucophyllum frutescens) surfaces under high impact velocity. No bounces were observed on both Eucalyptus (Corymbia) and Wild lettuce (Lactuca virosa) surfaces at low impact velocity due to low static contact angle. Under high impact velocity, however, splash and vibrational oscillations were identified on both Eucalyptus (Corymbia) and Wild lettuce (Lactuca virosa) surfaces.

ACKNOWLEDGMENTS

The authors are thankful to Central Instrumentation Facility Laboratory of Atmiya University for providing laboratory and instrumentation facility.

REFERENCES

1. Koishi T, Yasuoka K, Fujikawa S, and Zeng X C., Measurement of Contact-Angle Hysteresis for Droplets on Nanopillared Surface and in the Cassie and Wenzel States: A Molecular Dynamics Simulation Study, *ACS Nano*, v. 5, p. 6834-6842 (2011).
2. Marmur A., Wetting on Hydrophobic Rough Surfaces: To Be Heterogeneous or Not To Be? *Langmuir*, v. 19, p. 8343-8348 (2003).
3. Pogorzelski S J, Berezowski Z, Rochowski P and Szurkowski., A novel methodology based on contact angle hysteresis approach for surface changes monitoring in model PMMA-Corega Tabs system, *J. Appl. Surf. Sci*., v. 258, p. 3652-3658 (2012).
4. Balkenende A R, Van de Boogaard H J A P, Scholten M, and Willard N P., Evaluation of Different Approaches To Assess the Surface Tension of Low-Energy Solids by Means of Contact Angle Measurements, *Langmuir*, v. 14, p. 5907-5912 (1998).
5. Jung Y and Bhushan B., Dynamic Effects Induced Transition of Droplets on Biomimetic Superhydrophobic Surfaces, *Langmuir*, v. 25, p. 9208-9218 (2009).
6. Barbieri L, Wagner E and Hoffmann P L. Barbieri, E. Wagner and P. Hoffmann., Water Wetting Transition Parameters of Perfluorinated Substrates with Periodically Distributed Flat-Top Microscale Obstacles, *Langmuir*, v. 23, p. 1723-1734 (2007).
7. Jung Y and Bhushan B., Dynamic Effects of Bouncing Water Droplets on Superhydrophobic Surfaces, *Langmuir*, v. 24, p. 6262-6269 (2008).
8. Krasowska M, Krastev R, Rogalski M and Malysa K., Air-Facilitated Three-Phase Contact Formation at Hydrophobic Solid Surfaces under Dynamic Conditions, *Langmuir*, v. 23 p. 549–557 (2007).
9. Bertola V., Effect of polymer additives on the apparent dynamic contact angle of impacting drops, Colloids Surf. A:Physicochem, *Eng. Aspects*, v. 363, p. 135-140 (2010).
10. Yan Y Y, Gao N and Barthlott W., Mimicking natural superhydrophobic surfaces and grasping the wetting process: A review on recent progress in preparing superhydrophobic surfaces, *Adv. Colloid Interface Sci*., v. 169, p. 80-105 (2011).
11. Roach P, Shirtcliffe N J and Newton M I., Progress in superhydrophobic surface development, *Soft Matter*, v. 4, p. 224-240 (2008).

12. Lu X, Zhang W, Wang C, Wen T and Wei Y., One-dimensional conducting polymer nanocomposites: Synthesis, properties and applications *Progress in Polymer Science*, v. 36, p. 671-712 (2011).
13. Erbil H Y, McHale G, Rowan S M and Newton M I., Determination of the Receding Contact Angle of Sessile Drops on Polymer Surfaces by Evaporation. *Langmuir*, v. 15, p. 7378-7385 (1999).
14. Liu F P, Gardner D J and Wolcottg M P., A Model for the Description of Polymer Surface Dynamic Behaviour. Contact Angle vs Polymer Surface Properties. *Langmuir*, v. 11, p. 2674-2681 (1995).
15. Crick C R and Parkin I P., Water droplet bouncing-a definition for superhydrophobic surfaces. *Chem. Comm*., v. 47, p. 12059–12061 (2011).
16. Koch K, Bhushan B and Barthlott W., Hierarchically Sculptured Plant Surfaces and Superhydrophobicity. *Langmuir*, v. 25, p. 14116–14120 (2009).
17. Koch K, Bhushan B and Barthlott W., Multifunctional surface structures of plants: An inspiration for biomimetics. *Prog. Mat. Sci*., v. 54, p. 137-178 (2009).
18. Blossey R., Self-cleaning surfaces - virtual realities. *Nature Materials*, v. 2, p. 301-306 (2003).
19. Feng X, Gao X, Wu Z, Jiang L and Zheng Q., Superior Water Repellency of Water Strider Legs with Hierarchical Structures: Experiments and Analysis. *Langmuir*, v. 23, p. 4892-4896 (2007).
20. Fang Y, Sun G, Cong Q, Chen G and Ren L., Effects of Methanol on Wettability of the Non-Smooth Surface on Butterfly Wing. *Journal of Bionic Engineering*, v. 5, p. 127-133 (2008).
21. Byun D, Hong J, Saputra, Hwan Ko J, Lee Y J, Park H C, Byun B and Lukes J R., Wetting Characteristics of Insect Wing Surfaces., *Journal of Bionic Engineering*, v. 6, p. 63-70 (2009).
22. Münstedt H and Auhl D., Rheological measuring techniques and their relevance for the molecular characterization of polymers., *J. Non Newtonian Fluid Mech*., v. 128, p. 62-69 (2005).
23. Fitch R M., Rheology of molten polymers, London: Academic Press/Elsevier,57-72 (1997).
24. Fitch R M., Rheology of Polymer Colloids, London: Academic Press, 277-313 (1997).
25. Keller A A, Broje V and Setty K, Effect of advancing velocity and fluid viscosity on the dynamic contact angle of petroleum hydrocarbons., *Journal of Petroleum Science and Engineering*, v. 58, p. 201-206 (2007).
26. Callies M and Quéré D, On water repellency., *Soft Matter*., v. 1, p. 55-61 (2005).
27. Nosonovsky M and Bhushan B. Biomimetic Superhydrophobic Surfaces: Multiscale Approach., *Nano letters*., v. 7, p. 2633-2637 (2007).
28. Zhang X, Shi F, Niu J, Jiang Y and Wang Z. Superhydrophobic surfaces: from structural control to functional application., *J. Mater. Chem*., v. 18, p. 621-633 (2008).
29. Rioboo R, Voué M, Adão H, Conti J, Vaillant A, Seveno D, Coninck J., Drop Impact on Soft Surfaces: Beyond the Static Contact Angles., *Langmuir*, v. 26, p. 4873-4879 (2010).
30. Rioboo R, Voué M, Vaillant A and Coninck J. Drop Impact on Porous Superhydrophobic Polymer Surfaces., *Langmuir*., v. 24, p: 14074-14077 (2008).
31. Chen L, Xiao Z, Chan P, Lee Y and Li Z A., Comparative study of droplet impact dynamics on a dual-scaled superhydrophobic surface and lotus leaf, *Appl. Surf. Sci*., v. 257, p. 8857-8863 (2011).